Sains Malaysiana 49(11)(2020): 2735-2744
http://dx.doi.org/10.17576/jsm-2020-4911-12

A Tyrosine-Based Nanosensor for Rapid Sensitive Detection of Copper (II) Ions

(Pengesan Nano Berasaskan Tirosina untuk Pengesanan Sensitif Pantas Ion Tembaga (II))

JIAQI LIAN, PANDENG MIAO, NA LI, ABDUL JAMIL KHAN, XIANG JI* & FENG ZHANG

ABSTRACT

Most of the chromophores of fluorescent peptides contain aromatic amino acids with conjugated double bonds, among which tyrosine (Y) has become the focus of researches due to its unique physicochemical (optical, redox, and metal chelation) properties. However, there are few studies on the self-assembly and polymerisation of single. This study shows that the phenol group of Y can be oxidized into benzoquinone group in alkaline conditions and then undergoes polymerisation and further self-assembles into nanoparticles (NPs). The product of pY_{ox}*NPs have a strong fluorescence emission peak at 463 nm, and* Cu^{2+} *can spontaneously bind to it and dramatically quench their fluorescence. Based on these findings, we developed a rapid, sensitive and specific nanosensor for detecting* Cu^{2+}*. When the concentration of* Cu^{2+} *is within the range of 40* μM *- 1 mM, we can obtain a good linear correlation between the fluorescence intensity of* pY_{ox}*NPs and the concentration of copper ions, and the limit of detection (LOD) is determined to 37.26* μM*. In comparison to other modern methods for sensing* Cu^{2+}*, this method has advantages of simplicity of material synthesis, low cost, robust and rapid in sensing reaction, so we envision a good prospect for* Cu^{2+} *detection applications in both bulk and harsh environments.*

Keywords: Copper ion; fluorescence quenching; oxidation; polymerisation; tyrosine

ABSTRAK

Kebanyakan kromofor peptida pendarfluor mengandungi asid amino aromatik dengan ikatan berganda konjugasi, antaranya tyrosin (Y) telah menjadi tumpuan penyelidikan kerana ciri unik fizikokimianya (optik, redoks dan pengkelatan logam). Walau bagaimanapun, terdapat beberapa kajian mengenai pemasangan diri dan pempolimeran tunggal Y. Dalam kajian ini, kumpulan fenol Y boleh dioksidakan kepada kumpulan benzoquinon dalam keadaan alkali dan kemudian menjalani pempolimeran dan seterusnya menyambung diri ke nanozarah (NPs). pY_{ox}*NPs produk mempunyai puncak pelepasan pendarfluor yang kuat pada 463 nm dan* Cu^{2+} *secara spontan dapat mengikat mereka dan secara mendadak memadamkan pendarfluor mereka. Berdasarkan penemuan ini, kami membangunkan pengesan nano pesat, sensitif dan khusus untuk mengesan* Cu^{2+}*. Apabila kepekatan* Cu^{2+} *berada dalam julat 40* μM *- 1 mM, kita boleh mendapatkan korelasi linear yang baik antara keamatan pendarfluor* pY_{ox}*NPs dan kepekatan ion tembaga, dan had pengesanan (LOD) ditentukan kepada 37.26* μM*. Berbanding dengan kaedah moden yang lain untuk mengesan* Cu^{2+}*, ini memperlihatkan kelebihan dalam kesederhanaan sintesis bahan, kos rendah dan mudah diperoleh, cepat dan pantas dalam reaksi penderiaan, jadi kami membayangkan prospek yang baik untuk aplikasi pengesanan* Cu^{2+} *dalam persekitaran pukal dan mencabar.*

Kata kunci: Ion tembaga; pelindapkejutan pendarfluor; pengoksidaan; pempolimeran; tirosina

INTRODUCTION

Copper is one of the most important microelements in human body (Nieder et al. 2018). It mainly participates in the composition of enzymes in the organism and regulates the metabolism of both lipid and sugar (Baker et al. 2017; Kusunuru et al. 2013). However, excessive copper can cause poisoning (Bulcke et al. 2017).

Moreover, few mental illnesses such as schizophrenia and Alzheimer's disease (AD) are also related to copper ions (Cu^{2+}) (Brewer 2012; Yu et al. 2018). At present, the detection technology of Cu^{2+} mainly includes atomic absorption spectroscopy, colorimetry, fluorescence quenching and electrochemiluminescence analysis (Ghasemian et al. 2012). Among them, fluorescence-based methods attract great interest from researchers due to their outstanding advantages of fast response and high sensitivity. The traditional fluorescence-based methods mainly make use of organic dyes, and metal nanoclusters and inorganic quantum dots as chromophores (Li et al. 2017). Most of these chromophores are

difficult to synthesize, unstable or toxic, and are not environmentally-friendly (or biocompatible). Contino et al. (2016) used unoxidized L-tyrosine (Y)-coated silver nanoparticles (AgNPs) to detect Cu^{2+}; however, the instability of AgNPs significantly limits its applications due to easy oxidation. Xu et al. (2010) used colorimetric method to detect Cu^{2+} based on the gold nanoparticle (AuNP)-nucleotide (single strand) complex, in which three designed single-strand DNA can co-assemble to nanostructures, whose melting temperature (Tm) will increase with addition of Cu^{2+}, and this alteration is linear within a certain range of Cu^{2+} concentrations. However, this approach requires a time-consuming preparation. White and Holcombe (2007) used the Fmoc-based solid-phase synthesis method to produce peptides modified with a fluorescence chromophore of dansyl chloride, which can detect Cu^{2+} with their metal ion chelation capacity and then quench the fluorescence upon binding, however, the peptide synthesis is costly. Therefore, it is necessary to develop a new low-cost, simple and environment-friendly method for Cu^{2+} detection.

Peptide-based nanostructures are sensitive to the environmental conditions such as ionic strength, and temperature. Because of weak-intermolecular interactions such as van der Waals force, hydrophobic interaction, π-π stacking, electrostatic interaction, ionic and hydrogen bonds, their conformational changes will eventually cause the fluctuations of its inherent functionality, which usually is used to design sensors (Parmar et al. 2016). Hence, it would be great to construct fluorescent nanostructures using peptides or amino acids. However, to emit fluorescence in a visible light region is still a big challenge with peptide-based nanostructures. This is because natural amino acids such as phenylalanine (F), Y and tryptophan (W), can only emit fluorescence in the ultraviolet region (Teale & Weber 1957).

Previous studies have found that self-assembly of aromatic amino acids or short peptides can emit high-quantum-yield fluorescence in the visible light region (Pinotsi et al. 2016), in which probabilities for photo-radiation transition of electrons has been enhanced by decreasing the inactivation pathways (like thermal conversions) of activated electrons on the benzene ring, and meanwhile, the self-assembly enlarges the conjugated electron structures (Guo et al. 2019). Among these amino acids, Y has become the focus of researches because of its unique physicochemical properties and its importance in biological metabolism. For example, Y forms catecholamines under the action of enzymes (such as dopamine hydroxylase) *in vivo*, which has been found closely related to a mental disorder called attention deficit hyperactivity disorder (ADHD) in children (Bergwerff et al. 2016). Y can also form melanin under the action of tyrosinase, and the lack of tyrosinase can cause albinism (Kamaraj & Purohit 2014). At present, there have been many reports on the effects of nitration of Y and the Y residues of proteins, but few studies on the self-assembly and polymerisation of single Y molecules (Bartesaghi & Radi 2018).

In this study, aiming to build a biocompatible nanosensor for Cu^{2+} detection, we try to employ both polymerisation and self-assembly to produce fluorescent nanostructures using only Y, and further test it for Cu^{2+} sensing (Lin et al. 2011). In practice, we found that Y can be oxidized to its oxidized state Y_{ox} in alkaline solutions and further form polymer nanoparticles (pY_{ox}NPs) by both polymerisations of Y_{ox} and self-assembly, and the pY_{ox}NPs can emit stable and strong fluorescence, which can apply to sense Cu^{2+} due to their efficient quenching action (Figure 1).

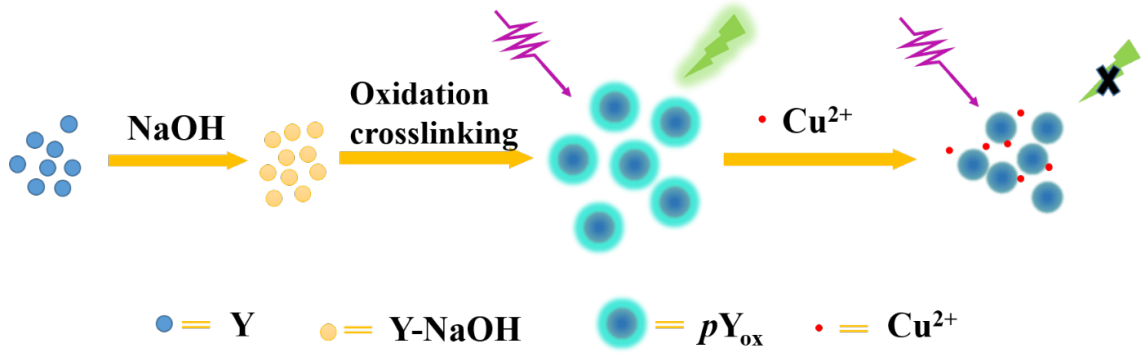

FIGURE 1. A schematic illustration of pY_{ox}NP construction and Cu^{2+} sensing. pY_{ox}NPs form by a combination of oxidation, polymerisation, and self-assembly in alkaline conditions. The purple arrows represent ultraviolet light, and the green 'thunder' represents fluorescence as excited by ultraviolet light. The blue fluorescence of pY_{ox}NPs can apply to Cu^{2+} sensing based-on an efficient quenching mechanism

Materials and Methods

Materials and Apparatuses

L-Tyrosine and all other reagents such as $CuCl_2$, $CaCl_2$, $CdCl_2$, $MgCl_2$, LiC_l, $NiCl_2$, $PbCl_2$, $ZnCl_2$, NaCl, and $AgNO_3$ metal ions were supplied by Aladdin Reagent Co. Ltd. (Shanghai, China); NaOH, HCl was supplied by Beijing Chemical Reagent Co. Ltd. (Beijing, China). All the metal ion compounds are analytical reagent grade without further purification. Deionized water (18.2 MΩ·cm) used for all experiments was made from a Milli-Q system (Millipore, Bedford, USA). All solvents were deionized water except for special descriptions. UV-Vis spectrometer (U-2900, Hitachi, Japan), Fluorescence spectrometer (Fluorolog®-MAX 4, Horiba, Japan), dynamic light scattering (DLS) equipment (Malvern Zetasizer Nano-ZS90, Malvern Instruments Ltd., UK).

Preparation of pY_{ox}NPs

Dissolved 72 mg of tyrosine in 20 mL of sodium hydroxide (0.1 M) and 20 mL of hydrochloric acid (0.1 M), respectively. Weighed 7.2 mg of tyrosine and dissolved it in 20 mL of water, heated it at 80 °C for condensation and refluxed for 4 h, then stopped heating and continue stirring overnight. After filtration with 0.22 μM membrane filters, we got the reserve solution of tyrosine dissolved in sodium hydroxide solution, i.e. synthetic polymerised oxidized Y NPs (pY_{ox}NPs), tyrosine hydrochloric acid solution reserve solution (Y-HCl), and tyrosine aqueous solution reserve solution (Y-H_2O), which was stored at room temperature. In addition, the particle size was measured by the DLS equipment (DLS), and the absorbance of the solution was measured with the ultraviolet visible spectrometer, the fluorescence spectra was recorded with the fluorescence spectrometer, and the solution fluorescence was observed under the UV lamp.

Assays for Sensing Cu^{2+}

Weighed 85.2 mg of cupric chloride dihydrate dissolved in 5 mL water to prepare a Cu^{2+} stock solution (100 mM), then gradually dilute it to obtain a concentration gradient as 10000, 7500, 5000, 2500, 1000, 750, 500, 250, 100, 75, 50, 25 μM. Took 100 μL of each gradient solution into the centrifuge tube and added 900 μL of oxidized tyrosine (Y_{ox}) stock solution, respectively, mixed and standed for 2 h. To measure fluorescence, the samples were excited at 365 nm, and the standard curve was made by plotting the fluorescence intensity at 463 nm against Cu^{2+} concentration. In order to determine the specificity of the method, we designed the interference experiment of other metal ions, and prepared metal ions solutions, such as: Zn^{2+}, Pb^{2+}, Ni^{+}, Na^{+}, Mg^{2+}, Li^{+}, Cd^{2+}, Ca^{2+}, Ag^{+} (100 μm). By treating these ions with the same method for Cu^{2+}, we can analyze the 'interference' of these ions on fluorescence. The limit of detection (LOD) was calculated according to the 3σ method.

Results and Discussion

Characterization of pY_{ox}NPs

To study the physicochemical properties, we obtained three Y-containing stock solutions, termed as pY_{ox}NPs, Y-HCl, and Y-H_2O. The stock solution of pY_{ox}NPs exhibits yellow colour, while stock solutions of Y-H_2O and Y-HCl are colourless. It is worth noting that the concentration of Y in water cannot be comparable to those in HCl and NaOH solutions, so to prepare Y-H_2O solution must be under the conditions of both heating and stirring overnight, the low water-solubility of Y is due to its natural chemical property (Li et al. 2019). In contrast, the preparation of Y-NaOH solution requires neither heating nor stirring overnight. For the other two solutions Y-H_2O and Y-HCl, a single peak at 274 nm shows in their absorption spectra (Figure 2(A)), indicating that Y is not oxidized. However, in the alkaline solution, the single absorption peak shifts to 293 nm and became bigger (Figure 2(A)), indicating the chemical changes of Y molecules. In terms of solution colour, the unheated Y-HCl solution is colourless and transparent, however, pY_{ox}NPs solution is yellow though still transparent, which could be due to the oxidation of hydroxyl groups on benzene ring under heating conditions, resulting in the change of liquid colour (Figure S1). In terms of molecular structure, deprotonation occurs to Y in alkaline solutions, producing groups like -COO- and -NH- (Figure S2), both of which enhance the solubility of Y. The blue fluorescence of pYox was observed using an excitation at 365 nm. The maximum emission peak was found at 463 nm in alkaline solutions (pYox), but not in the control solutions like Y-H2O, Y-HCL and Y-NaOH (Figure 2B). We speculate that a new additional ring (indoline structure) formed on the benzene ring of Y (Figure S2), creating a novel chromophore which makes the emission wavelength red-shifted (Lee et al. 2016).

According to the principle of fluorescence (Verlag 2006), some ground-state electrons outside the nucleus can be excited by the high energy of light, and then electron transition occurs. When this excited electron returns to the ground state, the energy will be released in the form of radiation to produce fluorescence. But not all energy can be released in the form of radiation, usually a small fragment of energy is released in the form of non-radiation like heat. When a single Y molecule absorbs UV light and its electrons firstly excited to high-energic orbitals and then they return to the ground state, some energy of the excited electrons will inevitably lose in a non-radiative transition way due to the rotational vibration of

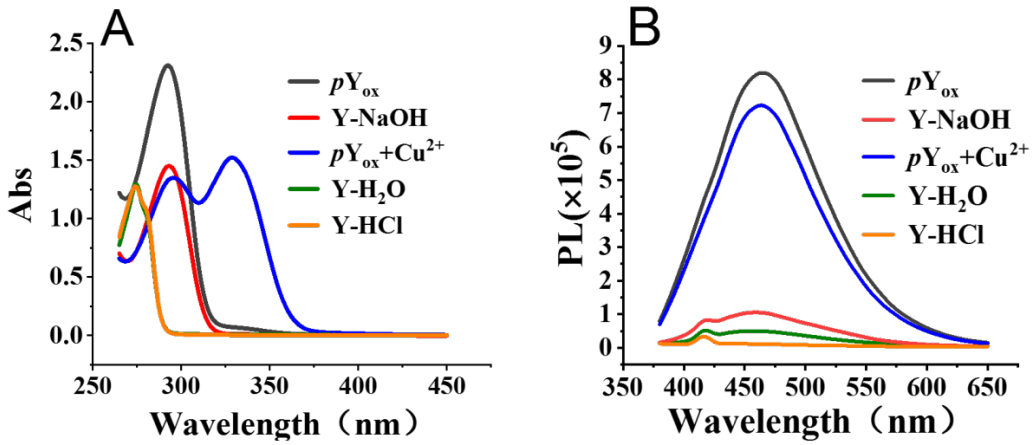

FIGURE 2. Optical characterization of Y under different conditions. Absorption A) and photoluminescence (PL). B) spectra of as-prepared Y samples in different conditions. pY_{ox}, the polymer of oxidized Y; Y-NaOH, the control solution of Y dissolved in diluted NaOH (without heating and reflux); pY_{ox} + Cu^{2+}, polymer of oxidized Y mixing with Cu^{2+}; Y-H_2O, Y just dissolved in water; Y-HCl, Y dissolved in dilute HCl solution; the detailed preparation can refer to the experimental section

the benzene ring, which will hardly produce fluorescence. Similar to GFP (Tsien 1998), the chromophore of GFP needs a β-barrel cage to lock its chromophore's rotation to improve its fluorescence quantum yield and meanwhile prevent water from quenching its fluorescence utilizing spatial isolation. After the cyclization and oxidation of Y residues, new chromophores were formed (Figure S2), which can be verified by the optical changes (Figure 2). After the oxidation and cross-linking of benzene rings (Figure S2), the chromophores were further locked to prevent rotating. All excited electrons should release energy via increased radiation-based transition, thus reduction radiation-based transition, eventually save energy for producing fluorescence (Figure 2) (Ren et al. 2019).

In order to proves that Y occurred crosslinking and polymerisation, DLS measurement was carried out. We observed that the hydrodynamic size of pY_{ox}NPs was about 5 nm, which is with following the normal distribution (Figure 3). If we increased the reflux time, we found that the hydrodynamic size pY_{ox} gradually increased (data not shown), indicating the extent of polymerisation/crosslinking. However, no matter if the reflux time is long or short, the DLS cannot obtain a good result for Y dissolved in HCl (Y-HCl) or water (Y-H_2O). However, because these solutions (Y-HCl and Y-H_2O) are colourless and transparent (Figure S1), indicating that Y is still dispersed in the solvent as a single molecule. Thus, the molecule is too small to be measured by the current DLS instrument, which further proves that Y does not occur oxidation and the successive cross-linking/polymerisation in acidic and neutral solutions.

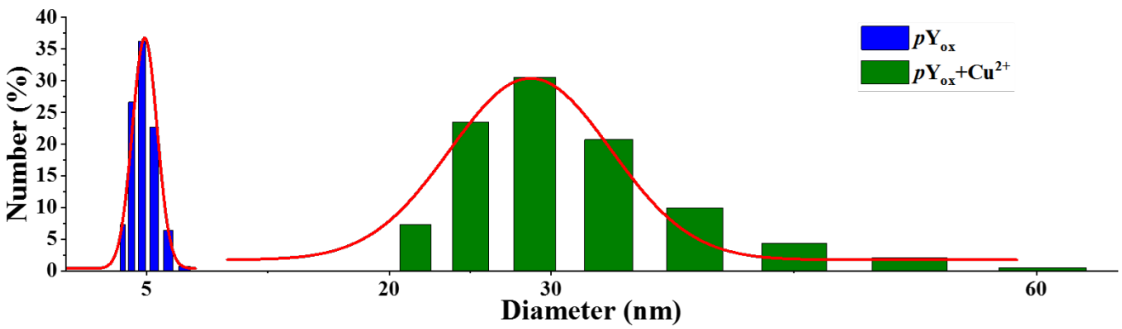

FIGURE 3. DLS analysis of the hydrodynamic size distribution of pY_{ox} before and after mixing with copper ions. The blue and green histograms represent pY_{ox} and pY_{ox} + Cu^{2+} samples, respectively. The red lines are the single peak fitting

pY_{ox}NPs emit blue fluorescence, which can be efficiently quenched upon binding with Cu^{2+} (pY_{ox}+ Cu^{2+}, Figure 2(B)). The size distribution of pY_{ox}NPs+ Cu^{2+} is measured to about 30 nm, which is significantly larger than that of pY_{ox}NPs themselves (Figure 3). With a new absorption peak appearing at 329 nm, we deduce that the cation ions can strongly coordinate with pY_{ox}NPs (Figure 2(A)). When the Cu^{2+} concentration is within the range of 25 μM - 10 mM, the fluorescence of pY_{ox}NPs at 463 nm decreases along with the increasing of Cu^{2+} concentration (Figure 4(A)). The plot of fluorescence intensity against the concentration of Cu^{2+} shows a shape of decay curve, so it was well fitted to an exponential decay function (Figure 4(B)) with the formula shown in (1) and (2).

$$y = 2.5 \times 10^5 - 3.4 \times 10^4 \times e^{\frac{t}{1.3\times10^2}} + 2.5 \times 10^5 \times e^{\frac{t}{1.0\times10^3}} + 3.4 \times 10^5 \times e^{\frac{t}{4.9\times10^3}} \quad (1)$$

$$t = 0.6 - x \quad (2)$$

When Cu^{2+} concentration ranges from 40 μM to 1 mM, the fluorescence intensity of pY_{ox}NPs changes linearly with Cu^{2+} concentration (Figure 5(A), S3(A)), with a linear equation, as shown in (3).

$$y = -209.44x + 8.6 \times 10^5 \ (R^2 = 0.9916) \quad (3)$$

The limit of detection (LOD) calculated by 3σ rule is 37.26 mM, which represents a relatively high sensitivity to Cu^{2+}. In addition, the Cu^{2+} quenching of the fluorescence of pY_{ox}NPs is also consistent with the Stern-Volmer equation (Figure S2), indicating a static quenching mechanism further proves the robust coordination between pY_{ox}NPs and Cu^{2+}.

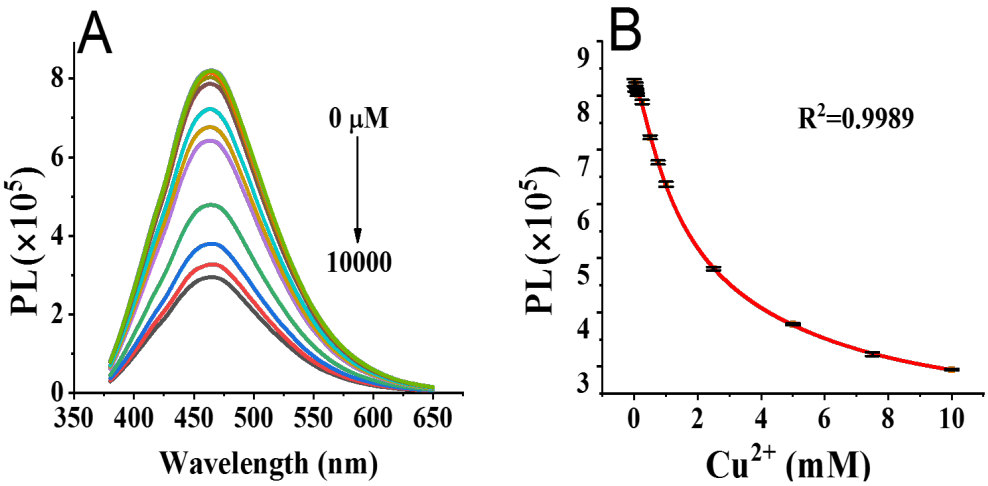

FIGURE 4. Sensing assays A) Fluorescence spectra of pY_{ox}NPs solutions mixed with gradient concentrations of Cu^{2+} as indicated in the figure (from upper to bottom, the concentration is increased), B) A plot of pY_{ox}NPs fluorescence intensity at 463 nm against Cu^{2+} concentration (black dots), and the corresponding fitting with a correlation coefficient (R2) of 0.9989

Taking other metal ions and Cu^{2+} of the same concentration for a comparison measurement, we analysed the interference of other metal ions on this method. The interference experiments of various common metal ions (100 μM) on the detection system showed that only Cu^{2+} had the best fluorescence quenching effect on pY_{ox}NP solution, while the other cations showed little effects on pY_{ox}NPs solution (Figure 5(B)), indicating a relatively high specificity for binding with Cu^{2+}.

Compared with other aromatic amino acids as fluorescent chromophores, the dopa quinone formed by oxidation of Y residues has redundant lone-pair electrons and is more likely to chelate metal ions (Lee & Lee 2015). Moreover, after crosslinking/polymerisation, the fluorescence of pY_{ox} solution exhibited a redshift, which could be due to the interactions of both hydrophobicity and π-π stacking. It is found that Cu^{2+} cannot make the pY_{ox}NPs aggregate and thus increase their hydrodynamic

sizes, but also strongly quench their fluorescence, which could be explained by the negative value of the Gibbs free energy ΔG (-16.27kJ/mol, see SI), indicating a spontaneous binding (Liu et al. 2015; Yuan et al. 2016; Zhong et al. 2014) between Cu^{2+} and pY_{ox}NPs.

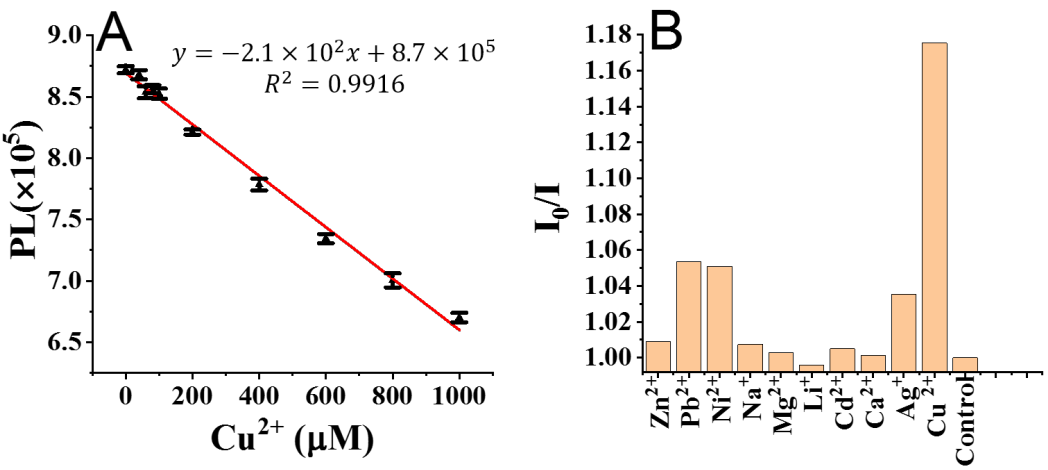

FIGURE 5. The optimized concentration ranges for sensing Cu^{2+} and the selectivity comparison of cations A) The plot of pY_{ox}NP fluorescence intensity at 463 nm against the Cu^{2+} concentration (black dots), and the corresponding linear fitting (red line) with a function and the correlation coefficient (R2), B) The selectivity or interference test of cations for pY_{ox}NPs-based sensor. I0 and I represent the 463 nm fluorescence intensity of pY_{ox}NPs in the absence and presence of cations

At last, we also assessed the reliability of the current developed approach, and the results are displayed in Table 1. By analysing the recoveries of Cu^{2+}, which varied from 104% to 112% with a relative standard deviation (RSD) ranging from 0.36 to 0.90, we think the results achieved by our method are in good agreement with the real values, indicating that the current sensing technology reported in this article are robust and reliable for sensing Cu^{2+} in aqueous solutions.

TABLE 1. Reliability evaluation of the Cu^{2+} sensing

Cu^{2+} samples	Added Cu^{2+} (μM)	Detected Cu^{2+} (μM)	RSD (n=5, %)	Recovery (%)
1	250	272.06	0.90	108.82
2	500	559.53	0.36	111.91
3	750	780.44	0.39	104.06

CONCLUSION

New technologies can inevitably innovate the living ways such as the clinical diagnosis in the contemporary era. The current fluorescent copper ion nanosensor was constructed via the combination of oxidation, polymerisation and self-assembly of single Y residues in basic conditions. We envision that co-assembling of more amino acids might create more versatile functional nanostructures, which hold great potential in bio-labeling/imaging/sensing, and even therapy for diseases. We also

believe this study will inspire scientists to open a new researching orientation based on the combination and co-assembling of amino acids via an artificial evolution way.

ACKNOWLEDGEMENTS

The following programs and foundations supported this work: the University Scientific Research Project of Inner Mongolia Autonomous Region (NJZC17267), the Program Funded by University for Fostering Distinguished Young Scholars, the National Natural Science Foundation of China (No.51763019, U1832125), the Grassland Talents Program of Inner Mongolia Autonomous Region, the Distinguished Young Scholars Foundation of Inner Mongolia Autonomous Region, and the Young Leading Talents of Science and Technology Program of Inner Mongolia Autonomous Region.

REFERENCES

Baker, Z.N., Cobine, P.A. & Leary, S.C. 2017. The mitochondrion: A central architect of copper homeostasis. *Metallomics* 9(11): 1501-1512.

Bartesaghi, S. & Radi, R. 2018. Fundamentals on the biochemistry of peroxynitrite and protein tyrosine nitration. *Redox Biol.* 14: 618-625.

Bergwerff, C.E., Luman, M., Blom, H.J. & Oosterlaan, J. 2016. No tryptophan, tyrosine and phenylalanine abnormalities in children with attention-deficit/hyperactivity disorder. *PLoS ONE* 11(3): e0151100.

Brewer, G.J. 2012. Copper excess, zinc deficiency, and cognition loss in Alzheimer's disease. *Biofactors* 38(2): 107-113.

Bulcke, F., Dringen, R. & Scheiber, I.F. 2017. Neurotoxicity of copper. *Adv. Neurobiol.* 18: 313-343.

Contino, A., Maccarrone, G., Zimbone, M., Reitano, R., Musumeci, P., Calcagno, L. & Oliveri, I.P. 2016. Tyrosine capped silver nanoparticles: A new fluorescent sensor for the quantitative determination of copper(ii) and cobalt(ii) ions. *J. Colloid Interface Sci.* 462: 216-222.

Ding, D., Guerette, P.A., Fu, J., Zhang, L., Irvine, S.A. & Miserez, A. 2015. From soft self-healing gels to stiff films in suckerin-based materials through modulation of crosslink density and beta-sheet content. *Adv. Mater*. 27(26): 3953-3961.

Ghasemian, E., Naghoni, A., Tabaraie, B. & Tabaraie, T. 2012. In vitro susceptibility of filamentous fungi to copper nanoparticles assessed by rapid xtt colorimetry and agar dilution method. *J. Mycol. Med.* 22(4): 322-328.

Ghosh, D. & Chattopadhyay, N. 2015. Gold and silver nanoparticles based super quenching of fluorescence: A review. *Journal of Luminescence* 160: 223-232.

Guo, J., Ramachandran, S., Zhong, R., Lal, R. & Zhang, F. 2019. Generating cyan fluorescence with de novo tripeptides: An in vitro mutation study on the role of single amino acid residues and their sequence. *ChemBioChem* 20(18): 2324-2330.

Hemmateenejad, B. & Yousefinejad, S. 2013. Interaction study of human serum albumin and ZNS nanoparticles using fluorescence spectrometry. *Journal of Molecular Structure* 1037: 317-322.

Kamaraj, B. & Purohit, R. 2014. Mutational analysis of oculocutaneous albinism: A compact review. *Biomed. Res. Int.* 2014: 905472.

Kusunuru, A.K., Tatina, M., Yousuf, S.K. & Mukherjee, D. 2013. Copper mediated stereoselective synthesis of c-glycosides from unactivated alkynes. *Chem. Comm.* 49(86): 10154-10156.

Lee, C. & Lee, S.Y. 2015. Mussel-inspired bolaamphiphile sticky self-assemblies for the preparation of magnetic nanoparticles. *Colloids Surf B Biointerfaces* 127: 89-95.

Lee, S., Liang, R., Voth, G.A. & Swanson, J.M. 2016. Computationally efficient multiscale reactive molecular dynamics to describe amino acid deprotonation in proteins. *J. Chem. Theory Comput.* 12(2): 879-891.

Li, M., Fu, Y. & Jin, L. 2017. A dual-signal sensing system based on organic dyes-LDHs film for fluorescence detection of cysteine. *Dalton Trans* 46(22): 7284-7290.

Li, X., Li, K., Farajtabar, A., He, Y., Chen, G. & Zhao, H. 2019. Solubility of d-tryptophan and l-tyrosine in several organic solvents: Determination and solvent effect. *Journal of Chemical & Engineering Data* 64(7): 3164-3169.

Lin, Y.W., Huang, C.C. & Chang, H.T. 2011. Gold nanoparticle probes for the detection of mercury, lead and copper ions. *Analyst* 136(5): 863-871.

Liu, Y-S., Zhang, P., Zhong, R., Bai, Z-J., Guo, J., Zhao, G-F. & Zhang, F. 2015. Fluorimetric study on the interaction between fluoresceinamine and bovine serum albumin. *Nuclear Science and Techniques* 26(3): 030505.

Nieder, R., Benbi, D.K. & Reichl, F.X. 2018. Microelements and their role in human health. In *Soil Components and Human Health*. Springer Netherlands, Dordrecht. pp. 317-374.

Parmar, A.S., James, J.K., Grisham, D.R., Pike, D.H. & Nanda, V. 2016. Dissecting electrostatic contributions to folding and self-assembly using designed multicomponent peptide systems. *J. Am. Chem. Soc.* 138(13): 4362-4367.

Pinotsi, D., Grisanti, L., Mahou, P., Gebauer, R., Kaminski, C.F., Hassanali, A. & Kaminski Schierle, G.S. 2016. Proton transfer and structure-specific fluorescence in hydrogen bond-rich protein structures. *J. Am. Chem. Soc.* 138(9): 3046-3057.

Ren, X., Zou, Q., Yuan, C., Chang, R., Xing, R. & Yan, X. 2019. Frontispiece: The dominant role of oxygen in modulating the chemical evolution pathways of tyrosine in peptides: Dityrosine or melanin. *Angewandte Chemie International Edition* 58(18): 5872-5876.

Teale, F.W. & Weber, G. 1957. Ultraviolet fluorescence of the aromatic amino acids. *Biochem. J.* 65(3): 476-482.

Tsien, R.Y. 1998. The green fluorescent protein**.** *Annu. Rev. Biochem.* 67: 509-544.

Verlag, S. 2006. *Principles of Fluorescence Spectroscopy.* New York: Plenum Press.

White, B.R. & Holcombe, J.A. 2007. Fluorescent peptide sensor for the selective detection of cu2+. *Talanta* 71(5): 2015-2020.

Xu, X., Daniel, W.L., Wei, W. & Mirkin, C.A. 2010. Colorimetric $Cu^{(2+)}$ detection using DNA-modified gold-nanoparticle aggregates as probes and click chemistry. *Small* 6(5): 623-626.

Yu, H., Wang, D., Zou, L., Zhang, Z., Xu, H., Zhu, F., Ren, X., Xu, B., Yuan, J., Liu, J., Spencer, P.S. & Yang, X. 2018. Proteomic alterations of brain subcellular organelles caused

by low-dose copper exposure: Implication for Alzheimer's disease. *Archives of Toxicology* 92(4): 1363-1382.

Yuan, M., Zhong, R., Yun, X., Hou, J., Du, Q., Zhao, G. & Zhang, F. 2016. A fluorimetric study on the interaction between a Trp-containing beta-strand peptide and amphiphilic polymer-coated gold nanoparticles. *Luminescence* 31(1): 47-53.

Zhong, R., Liu, Y., Zhang, P., Liu, J., Zhao, G. & Zhang, F. 2014. Discrete nanoparticle-BSA conjugates manipulated by hydrophobic interaction. *ACS Applied Materials & Interfaces* 6(22): 19465-19470.

Jiaqi Lian, Xiang Ji1* & Feng Zhang*
School of Life Science and Technology
Inner Mongolia University of Science and Technology
Baotou 014010
P. R. China

Jiaqi Lian, Pandeng Miao, Na Li, Abdul Jamil Khan & Feng Zhang*
Biomedical Nanocenter, School of Life Science
Inner Mongolia Agricultural University
Hohhot 010018
P. R. China

Pandeng Miao & Na Li
Terahertz Technology Innovation Research Institute
Shanghai Key Laboratory of Modern Optical System
Terahertz Science Cooperative Innovation Center
University of Shanghai for Science and Technology
516 Jungong Road, Shanghai 200093
P. R. China

Feng Zhang*
Key Laboratory of Oral Medicine
Guangzhou Institute of Oral Disease
Stomatology Hospital, Department of Biomedical Engineering
School of Basic Medical Sciences
Guangzhou Medical University
Guangzhou 511436
P. R. China

*Corresponding author; email: jixiang@imust.cn

Received: 17 January 2020
Accepted: 8 June 2020

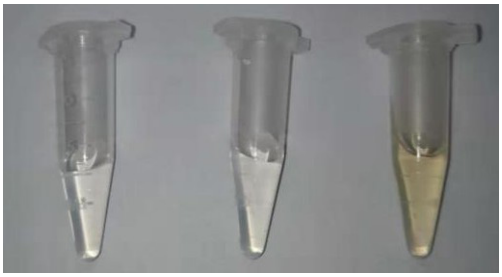

FIGURE S1. The color comparison of Y-HCl, Y-H_2O and pY_{ox} solutions (from left to right) under daylight

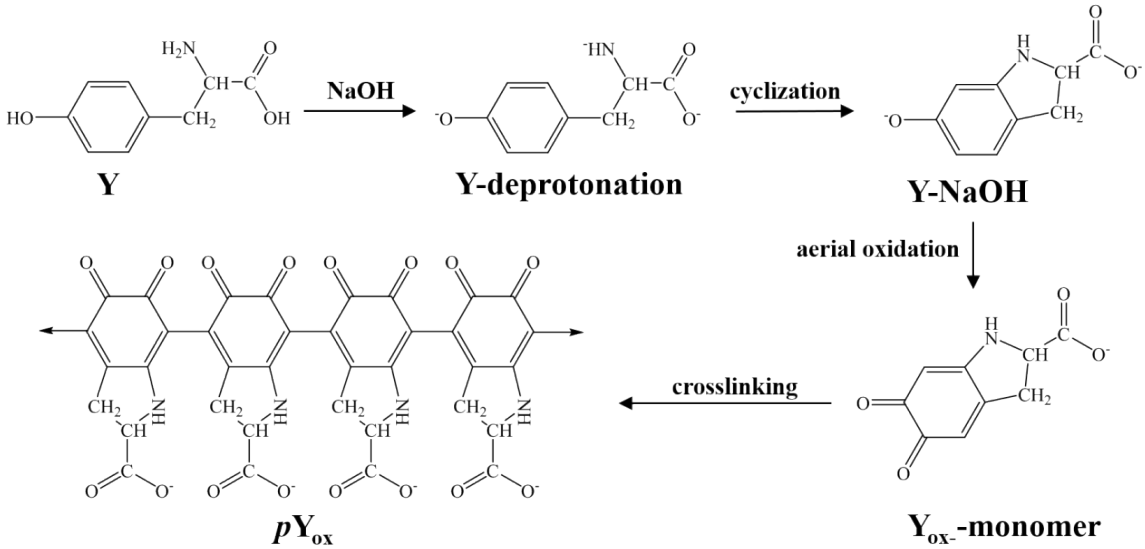

FIGURE S2. A chemical evolution procedure of Y in alkaline solutions. In sodium hydroxide solution, Y can be firstly deprotonated to produce imine group (-NH^-), deprotonated hydroxyl group (-O^-) and carboxylic group (-COO^-), and then the imine group and benzene ring can cyclize to form a two-ring structure (indoline group, whose absorption peak shifts to red region), then hydroxyl groups are further oxidized to form O-benzoquinone (Y_{OX}), which eventually polymerize to pY_{OX} by cross-linking reaction (Ding et al. 2015)

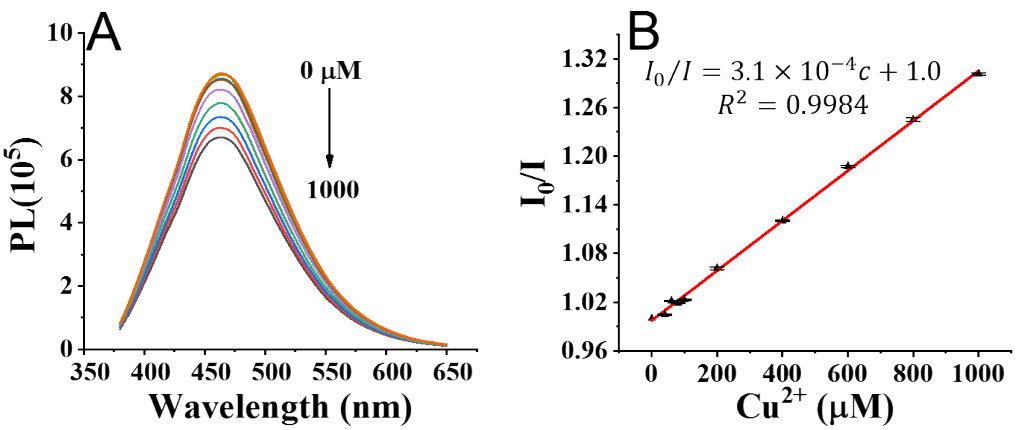

FIGURE S3. The assays of pY_{OX}NPs, fluorescence quenched by Cu^{2+} A). The steady-state fluorescence spectra of pY_{OX}NPs mixed with various concentrations of Cu^{2+} ranging from 0 to 1000 μM as indicated by the arrow in the figure. The spectra were recorded at 298 K with an excitation of 365 nm, B) The Stern-Volmer plot (black dots) for the fluorescence quenching ratio of pY_{OX} against Cu^{2+} ion (black dots) and the corresponding linear fitting (red line). I0 and I represent the fluorescence intensity of the pY_{OX}NP solution before and after mixing with different concentrated Cu^{2+}

FLUORESCENCE QUENCHING AND THERMODYNAMICS

In order to figure out the mechanism how Cu^{2+} can quench pY_{ox}NPs, we studied the thermodynamics of this binding system, in which the quencher is Cu^{2+}. According to the Stern-Volmer equation (Ghosh & Chattopadhyay 2015) (1), in which I0 and I are the fluorescence intensities in presence and absence of quenchers, respectively. [Q], K_{SV} and τ_0 are the concentration of quencher, the quenching constant of Stern-Volmer and the life time of fluorescence, respectively.

$$\frac{I0}{} = K_{SV}[Q] + 1 \quad \text{(S1)}$$

$$K_{SV} = K_q \times \tau_0 \quad \text{(S2)}$$

Generally, the quenching constant K_q is used to better describe this process. And all the τ_0 of biomolecules can be considered as 10^{-8} s, therefore, if using the quenching constant (Kq, (2)) to replace K_{SV} in (1), we can obtain $K_{SV} = 3.1 \times 10^2\ M^{-1}$ and $Kq = 3.1 \times 10^{10}\ M^{-1}.\ S^{-1}$. Because the K_q is bigger than the diffusion-controlled limit (normally near $1 \times 10^{10}\ M^{-1}.\ S^{-1}$), therefore, we think pY_{ox}NPs and Cu^{2+} involve static binding.

In order to verify this reaction can occur spontaneously, we also calculate the Gibbs free energy ΔG (Hemmateenejad & Yousefinejad 2013). By using the Hill equation (S3) in which I_{sat}, η and K_α refer to the fluorescence intensity of pY_{ox}NPs mixed with a saturated amount of Cu^{2}+, Hill coefficient and the binding constant, respectively.

$$\log[I_0 - I\ I - I_{sat}] = \log K_\alpha + n \log[Q] \quad \text{(S3)}$$

The K_α was calculated to 7.1×10^2 (M^{-1}), with which the ΔG can be calculated to $-1.6 \times 10^1 kJ{\cdot}mol^{-1}$ (S4).

$$\Delta G = -RT \ln K_\alpha \quad \text{(S4)}$$

Because the $\Delta G < 0$, therefore, the binding between Cu^{2+} and pY_{ox}NPs should be spontaneous.